

MRI-guided Transurethral Ultrasound Therapy of the Prostate Gland Using Real-time Thermal Mapping: Initial Studies

Kashif Siddiqui, Rajiv Chopra, Siddharth Vedula, Linda Sugar, Masoom Haider, Aaron Boyes, Mireia Musquera, Michael Bronskill, and Laurence Klotz

OBJECTIVE

To confirm the correlation between planning and thermal injury of the prostate as determined by magnetic resonance imaging (MRI) and histology in canine and humans treated with transurethral ultrasound.

MATERIAL AND METHODS

Canine studies: 2 sets of in vivo studies were performed under general anesthesia in 1.5 T clinical MRI. Nine dogs were treated using single transducer; 8 dogs were treated using urethral applicator with multiple transducers. Rectal cooling was maintained. After initial imaging, a target boundary was selected and high-intensity ultrasound energy delivered. The spatial temperature distribution was measured continuously every 5 seconds with MR thermometry using the proton-resonant frequency shift method. The goal was to achieve 55 °C at the target boundary. After treatment, the prostate was harvested and fixed with adjoining tissue, including rectum. Temperature maps, anatomical images, and histologic sections were registered to each other and compared.

Human studies: To date, 5 patients with localized prostate cancer have been treated immediately before radical prostatectomy. Approximately 30% of the gland volume was targeted.

RESULTS

A continuous pattern of thermal coagulation was successfully achieved within the target region, with an average spatial precision of 1-2 mm. Radical prostatectomy was routine, with an uncomplicated postoperative course in all patients. The correlation between anatomical, thermal, and histologic images was ≤ 3 mm. Treatment time was < 30 minutes. No thermal damage to rectal tissue was observed.

CONCLUSIONS

Thermal ablation within the prescribed target of the prostate has been successfully demonstrated in canine studies. The treatment is also feasible in humans. UROLOGY 76: 1506–1511, 2010. © 2010 Elsevier Inc.

Existing therapies for prostate cancer have significant long-term morbidities.¹ There is, thus, great interest in developing an image-guided, minimally invasive treatment that achieves comparable cancer cure rates with fewer complications.²

Magnetic resonance imaging (MRI)-guided transurethral ultrasound therapy is a novel, minimally invasive approach developed by Imaging Research at Sunnybrook Health Sciences Centre in collaboration with the Department of Urology. This technology generates a controlled pattern of irreversible thermal injury in the prostate. The procedure is performed in a clinical MR imager, enabling real-time temperature feedback during treatment for precise and efficient coagulation. The spatial accuracy and speed

with which this therapy can be delivered hold promise for application in treatment of low- and intermediate-risk prostate cancer patients,^{3,4} as well as in those with benign prostatic hyperplasia. It could also have potential for use in salvage situations of locally recurrent/persistent prostate cancer cases with previously failed treatment and/or rising prostate-specific antigen (PSA).

Previous investigations have demonstrated the feasibility of monitoring temperature in the prostate gland with MRI during laser⁵ and microwave⁶ thermal therapy. However, to date, no studies have investigated real-time MR temperature feedback in vivo to generate precise patterns of thermal damage in the prostate gland. We report the correlation between the initial planning and thermal injury as determined by MRI and subsequent evidence of tissue necrosis on histology in a canine model. Preliminary results from an ongoing human feasibility study in patients with clinically localized (confined to prostate gland) prostate cancer scheduled for radical prostatectomy are also described.

From the Departments of Urology, Imaging Research, Pathology, Radiology, and Medical Biophysics, University of Toronto, Sunnybrook Health Sciences Centre, Toronto, Ontario, Canada

Corresponding author: Kashif Siddiqui, F.R.C.S.(Urol), F.E.B.U., M.M.S., University of Toronto, Sunnybrook Health Sciences Centre, 2075 Bayview Avenue, Toronto, Ontario M4N 3M5, Canada. E-mail: kashifsiddiqui2@gmail.com

MATERIAL AND METHODS

The MRI-compatible system, which has been tested in both 1.5 and 3.0 T MRI consists of a brass transurethral applicator incorporating planar transducers, rotational (360°) positioning system, radiofrequency electronics, and urethral and rectal flow circuits.⁷ Thermal coagulation within a targeted region of the prostate was achieved by generating temperatures of approximately 55 °C along a prescribed target boundary by continuous rotation of the urethral applicator, producing ultrasound fields extending radially.

Spatial accuracy of heating was achieved by real-time temperature feedback. MRI scans were acquired at the location of the transducer with a temporal resolution of 5 seconds and a spatial resolution of 1.5 mm (in plane) × 5-10 mm (slice thickness). The images were obtained using a standard gradient echo acquisition, and quantitative temperature maps were calculated using the proton resonant frequency shift (PRFS) method.⁸ Multiple planes can be acquired within the 5-second imaging window, enabling measurement of the 3D heating pattern in the prostate during treatment. The temperature maps were processed immediately after acquisition by custom-written software interfaced to the MRI. A control algorithm implemented in this software adjusted the output power, frequency, and rotation rate of the device based on these temperatures and the target boundary. At a given point of time, the principal temperature control point is located at the target boundary along the direction of the beam. Furthermore, the controller also caps the maximum temperature along the direction of the beam at 90 °C to ensure that no tissue boiling occurs. As the applicator is rotated, the control point is changed to remain along the direction of the ultrasound beam. This method of temperature feedback was shown to produce conformal patterns of heating in prostate geometries in the presence of realistic MRI parameters in our previously published simulation and phantom studies.^{9,10}

Canine Studies

Two sets of experiments were performed under general anesthesia with the animals placed supine in 1.5 T clinical MRI (GE Healthcare, Waukesha, WI). In the first group of 9 dogs (5 acute and 4 delayed), applicators with a single transducer (3.5 × 15 mm) operating at 9.1 MHz and 7.5-W maximum acoustic power were used; in the second group, 8 dogs were treated using multiple transducers (4 × 3.5 × 5 mm) operating at 8 MHz and maximum acoustic power of 1.75 W (10 W/cm²) simultaneously, to coagulate larger volumes of tissue. Urethral applicators were inserted through perineal urethrostomy. In general, ultrasound parameters were based on our simulation studies. The radial distance from the applicator to the target boundary ranged between 7 and 20 mm for single transducer experiments and between 10 and 18 mm in each treatment plane of the multiple transducer studies. For histologic reasons, target boundaries were typically shaped to the prostate at least 3 mm inside the prostate boundary leading to various target volumes based on individual canine prostate size and geometry. The target boundary was recorded in the MRI scans and the boundary for thermal coagulation was measured on the hematoxylin and eosin-stained slides (whole-mount) after processing. These were compared with each other after registering the prostate tissue section and the imaging slice. The section was obtained from the same location as the treatment.

The mixed breed dogs weighing 27-38 kg were selected to treat large prostates representative of human prostate sizes. Rectal cooling was maintained at 20 °C by water (doped

with MnCl₂ to remove the signal and potential artifacts) flowing through an endorectal cooling device. A urethral flow circuit circulated water at 37 °C for cooling the transducers. Active cooling for preservation of the urethra was not implemented in these studies. All animals were given a rectal enema before being sedated and intubated. All experiments were performed in an acute model (prostate harvested immediately after treatment) except for 4 dogs in the first group that were allowed to recover for 48 hours after treatment to assess any delayed effects. The 48-hour period was chosen because of restrictions from our institutional Animal Care Committee and also because the healing process in the canine prostate is relatively unimpeded and achieved in a short period.¹¹ Approval for these experiments was obtained from the institutional Animal Care Committee and funding was obtained from the Terry Fox Foundation and the Ontario Institute for Cancer Research.

After initial T2-weighted anatomical imaging transverse to the applicator plane, an arbitrary target boundary was selected and treatment delivered. Intravenous Buscopan (20 mg/mL; Boehringer Ingelheim GmbH, Germany) was given just before starting the treatment to overcome any colonic or rectal peristalsis that might cause artifacts and interfere with thermometry. The spatial temperature distribution was measured continuously using the PRFS method¹² achieving temperature resolution of ±1 °C updated every 5 seconds. Contrast-enhanced and T2-weighted images were acquired after treatment and repeated at 48 hours in the delayed group.

The prostate was harvested with adjoining tissue, including rectum, and serially sectioned using a thin (250-μm) Histotech (Vibratome, Bannockburn, IL) blade aligned transversely to a plastic rod (0.25" Derlin; DuPont, Wilmington, DE) inserted in place of the applicator in the urethra, corresponding to the MRI plane. Tissue sections were fixed in 10% neutral buffered formalin for at least 10 days before obtaining the whole-mount histologic sections by microtome sectioning at 5 μm and staining with hematoxylin and eosin. To ensure consistency of pathologic diagnosis, all tissue sections were reviewed by the same uropathologist who demarcated the regions of complete thermal damage (100% cell kill) and no damage (0% cell kill). Image registration techniques developed in-house were used for comparison of thermal, anatomical, and histologic images.

Human Studies

To date, 5 patients with cancer confined to the prostate have volunteered for testing this technology immediately before their scheduled radical prostatectomy. Approval from the institutional Research Ethics Board and informed consent from the patients were obtained. The transurethral ultrasound treatment was performed in a clinical MRI scanner under spinal anesthesia the morning before surgery. Preoperative preparation was the same as for radical prostatectomy. The bladder was emptied using a 16-F Foley catheter just before insertion of the device. With technical feasibility as our goal, small volumes up to 30% of the prostate were targeted. All patients had PSA <15 ng/mL, clinical stage T1/T2a disease, and Gleason score of ≤7 (3 + 4) on prostate biopsies within the previous 6 months.

RESULTS

The nature of thermal mapping acquired in real-time continuously during a typical treatment is shown as a

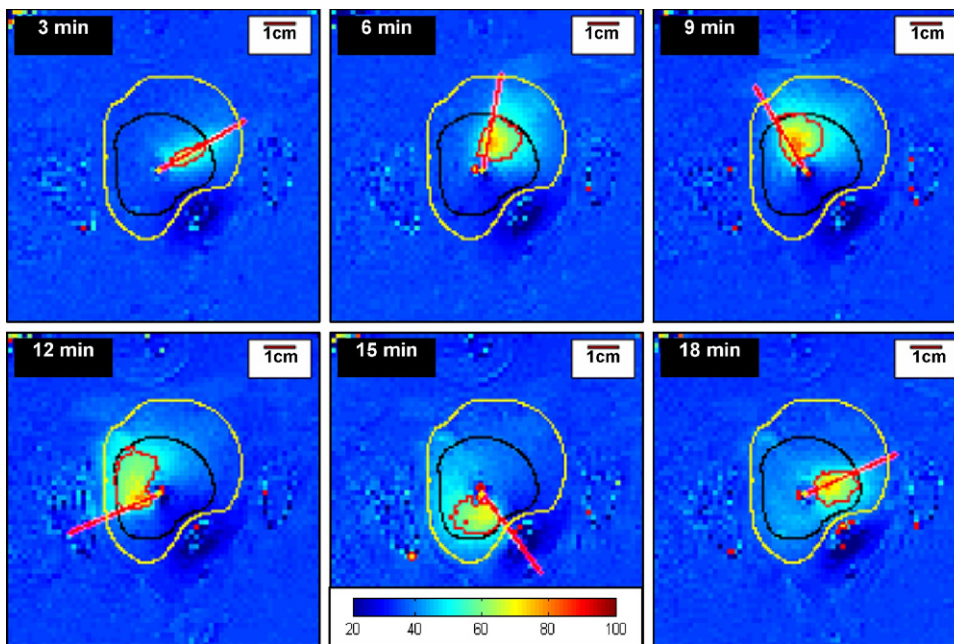


Figure 1. MR temperature images (5-second) shown every 3 minutes during MRI-guided transurethral ultrasound treatment of a canine prostate. Prostate boundary in yellow, target boundary in black, and heated area delineated with the 55° isotherm marked in red. The straight red line shows the direction of the urethral applicator during this counter-clockwise rotation.

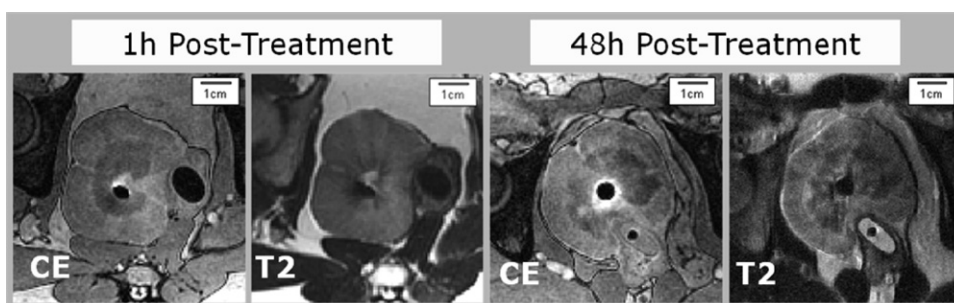


Figure 2. Typical post-treatment contrast-enhanced (CE) and T2-weighted MRI scans illustrating the thermal damage pattern from transurethral ultrasound treatment in an acute model and a delayed model. The coagulation region is immediately apparent only in CE images but, at 48 hours, is clear in both types of MRI scans.

series of 5-second MRI temperature images at different time intervals in Figure 1. In this figure, the capability and coverage of the device rotation system as it adjusts dynamically to the prostate geometry for delivery of ultrasound energy can be seen from the temperature distribution within the target region at different times during treatment. Temperature in the rectum is low because of cooling. The maximum temperature reached during treatment was well within the target boundary. Similar results were seen for all animals.

The thermal damage pattern was evident from contrast-enhanced images taken shortly after treatment in the acute model and at 48 hours in the survival group, as shown in Figure 2. Histologic analysis confirmed coagulative necrosis with the presence of shrunken pyknotic nuclei and brightly eosinophilic granular cytoplasm with interstitial hemorrhage within the treated region, as reported previously.¹³ An area of transition characterized

by retained basic gland structure but altered epithelium was seen between the coagulated and normal-appearing regions in acute studies, which may be attributable to temperatures below the threshold for coagulation with rapid recovery to normal, which has also been demonstrated in studies of similar nature.¹¹ The maximum dimension of this transition zone in any direction in all of the experiments did not exceed 3 mm (mean 1.28 ± 0.49 mm). Sharp demarcation between coagulated and normal tissue was seen at 48 hours.

The targeting accuracy was measured as the precision by which 55 °C isotherm was achieved at the target boundary using a scatter-plot analysis. Figure 3 shows a scatter plot of radial distance of the 55 °C isotherm from the device versus the corresponding target boundary radius for both single- and multiple-transducer studies. A perfect treatment would be embodied as a result where all points fell along a diagonal line with unity slope. It can

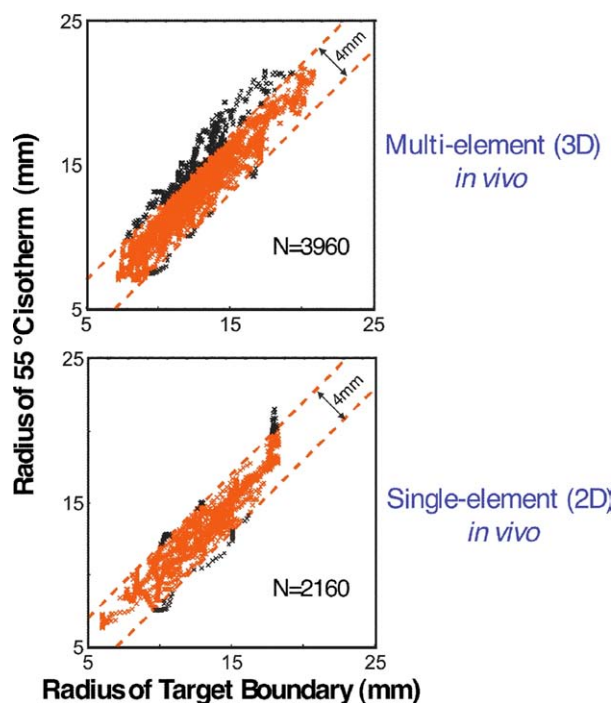


Figure 3. Targeting accuracy of 55° isotherm to target boundary in transurethral ultrasound treatment for single- and multiple-transducer canine studies. N = number of data points in all experiments. For comparison, the pixel size in the MR temperature images was 1.56×3.13 mm.

be seen that, in general, the target isotherm was reached within ± 2 mm of the target on either side, with a mean of 0.6 ± 1.1 mm for multi-element and 0.2 ± 1.0 mm for single-element studies. The pixel size in the temperature images was 1.56×3.13 mm. The spatial and temporal accuracy of heating in the prostate using single transducers has been previously reported by our group using different analysis techniques.¹⁴

The treatment accuracy was measured as the precision with which histologic coagulation was achieved compared with the target boundary, as shown in Figure 4. In most cases, histologic coagulation was achieved within 2 mm of the target. However, errors of up to 3 mm were seen mostly at shorter target radii (< 10 mm), where temperature artifacts and registration error is much larger. The mean error for multi-element was 0.8 ± 2.0 mm and 0.6 ± 2.0 mm for single-element studies.

The entire treatment took less than 30 minutes in all studies. There was spontaneous voiding with no distress noted in the survival group during the 48-hour recovery period. No thermal damage outside the prostate was noted in any study. No damage to the rectum was found.

The ongoing feasibility study in men is currently recruiting patients. The concept has been well received and treatment tolerated well by all patients. No issues with device placement or patient movement during treatment have been encountered. Radical prostatectomy im-

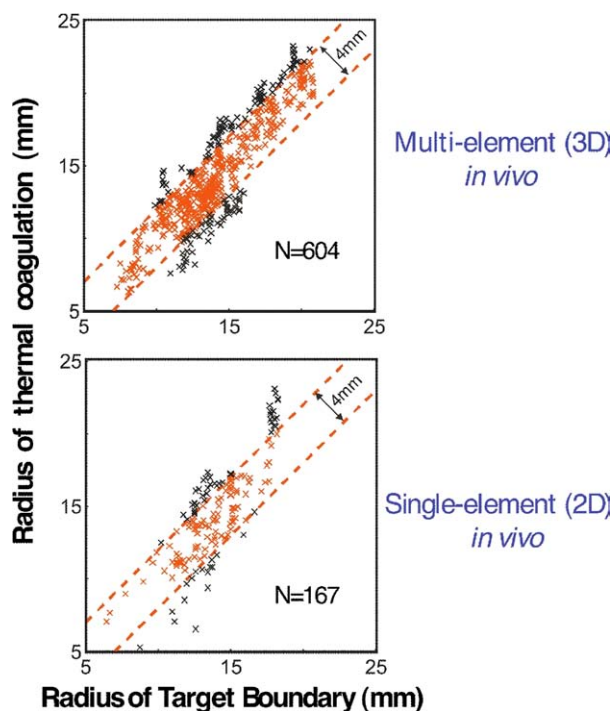


Figure 4. Treatment accuracy of histologic measurement to target boundary in transurethral ultrasound treatment for single- and multiple-transducer canine studies. N = number of data points in all experiments.

mediately after treatment has been as usual. No thermal changes have been noticed in the tissues around the prostate.

COMMENT

Hyperthermia ($> 40^\circ\text{C}$) can be delivered alone or as an adjunct to radiation and/or chemotherapy to treat cancer. Higher temperatures have a direct cytotoxic effect on cells and delivery of target temperatures above 46°C is defined as thermoablation.¹⁵ The canine prostate, a bilobed structure, is affected by cancer in 5%-7% of prostatic disease cases and usually presents late with symptoms of local or regional metastasis, making it extremely difficult to assess the effects of any treatment modality on carcinomatous tissue.¹⁶ Various techniques like transrectal high-intensity focused ultrasound (HIFU), interstitial microwave ablation, and transurethral microwave thermal therapy have been used successfully to cause irreversible, homogenous coagulative necrosis in benign^{17,18} and malignant prostate conditions.^{19,20} Although these approaches have achieved the desired temperatures, they have significant limitations in terms of inability to visualize the spatial heating pattern during treatment, long treatment times, and limited control over the distribution of energy. Safety and efficacy of thermal therapy require accurate temperature measurement throughout the procedure. Tissue motion during scanning and between consecutive images is the most prevalent problem of MR thermometry.^{21,22} In addition, flowing water and

blood can also be misinterpreted as temperature changes, causing artifacts. We did not observe blood flow to cause major artifacts in the prostate and water was doped with 10 mM of $MnCl_2$ to eliminate the proton signal. Respiration has little effect on pelvic organs like the prostate, which in this case was further immobilized by presence of the applicator.

Ultrasound has shown considerable promise in its ability to produce more precise and deeper thermal foci.²³ The nonionizing nature of ultrasound enables repeated treatment if required. In our approach, the ultrasound beam sweeps across the target region continuously, which is different from transrectal HIFU, which involves delivering many individual sonications in a raster fashion, each separated in time by a cooling interval.²⁴ The dramatic temperature rise at the point of focus in HIFU causes coagulation of a small tissue volume (1-3 mm wide, 5-20 mm high), requiring placement of elementary focal lesions side-to-side throughout the target region.²⁵ The delivery of HIFU from within the prostate, as in the transurethral route, avoids passing energy through the rectal wall, which eliminates the need to implement extended cooling time, reducing overall treatment time significantly²⁶ and potentially reduces the chances of few but significant rectal complications.²⁷ The transurethral approach is also amenable to delivery in a clinical MRI, with fewer technical challenges compared with the transrectal route, enabling real-time temperature feedback during treatment and accurate assessment of the treated area with gadolinium-enhanced scans afterward.

Our study demonstrates targeting and treatment accuracy using a multi-element applicator that can treat a larger gland volume. Our analysis confirms that, within error, the more complex multi-element treatments work just as well as the simple single-element treatments.

Further improvements of the control algorithm to incorporate urethral preservation and dual frequency transducers in whole-gland treatment are being tested in phantoms and canines where detailed histologic analysis of urethra, rectum, and other adjoining vital structures is being carried out with improved image registration, which we believe is vital for the next stage of phase I human trials.

CONCLUSIONS

MRI-guided transurethral ultrasound therapy using real-time temperature feedback enables precise and rapid thermal ablation of the canine prostate. The ongoing feasibility study in humans will investigate the tolerability and capability for treating the human prostate. This approach has obvious applications in the treatment of localized prostate cancer.

References

1. Potosky AL, Davis WW, Hoffman RM, et al. Five-year outcomes after prostatectomy or radiotherapy for prostate cancer: the Prostate Cancer Outcomes Study. *JNCI*. 2004;96(18):1358-1367.
2. Eggener SE, Scardino PT, Carroll PR, International Task Force on Prostate Cancer, et al. And the focal lesion paradigm. Focal therapy for localized prostate cancer: a critical appraisal of rationale and modalities. *J Urol*. 2007;178(6):2260-2267.
3. Shinohara K. Thermal ablation of prostate diseases: advantages and limitations. *Int J Hyperthermia*. 2004;20(7):679-697.
4. Pauly KB, Diederich CJ, Rieke V, et al. Magnetic resonance-guided high-intensity ultrasound ablation of the prostate. *Top Magn Reson Imaging*. 2006;17(3):195-207.
5. Peters RD, Chan E, Trachtenberg J, et al. Magnetic resonance thermometry for predicting thermal damage: an application of interstitial laser coagulation in an in vivo canine prostate model. *Magn Reson Med*. 2000;44(6):873-883.
6. Chen JC, Moriarty JA, Derbyshire JA, et al. Prostate cancer: MR imaging and thermometry during microwave thermal ablation—initial experience. *Radiology*. 2000;214(1):290-297.
7. Chopra R, Baker N, Choy V, et al. MRI-compatible transurethral ultrasound system for the treatment of localized prostate cancer using rotational control. *Med Phys*. 2008;35:1346-1357.
8. McDannold N. Quantitative MRI-based temperature mapping based on the proton resonant frequency shift: review of validation studies. *Int J Hyperthermia*. 2005;21(6):533-546.
9. Chopra R, Wacksmuth J, Burtnyk M, et al. Analysis of factors important for transurethral ultrasound prostate heating using MR temperature feedback. *Phys. Med Biol*. 2006;51:827-844.
10. Chopra R, Burtnyk M, Haider MA, et al. Method for MRI-guided conformal thermal therapy of prostate with planar transurethral ultrasound heating applicators. *Phys. Med Biol*. 2005; 50:4957-4975.
11. Pow-Sang M, Oriheula E, Motamedi M, et al. Healing response of the canine prostate to Nd: YAG laser radiation. *Prostate*. 1996;28: 287-294.
12. Scheffler K. Fast frequency mapping with balanced SSFP: theory and application to proton-resonance frequency shift thermometry. *Magn Reson Med*. 2004;51(6):1205-1211.
13. Boyes A, Tang K, Yaffe M, et al. Prostate tissue analysis following magnetic resonance imaging guided transurethral ultrasound thermal therapy. *J Urol*. 2007;178:1080-1085.
14. Chopra R, Tang K, Burtnyk M, et al. Analysis of the spatial and temporal accuracy of heating in the prostate gland using transurethral ultrasound therapy and active MR temperature feedback. *Phys. Med Biol*. 2009;54:2615-2633.
15. Hildebrandt B, Wust P, Ahlers O, et al. The cellular and molecular basis of hyperthermia. *Crit Rev Oncol/Hematol*. 2002; 43(1):33-56.
16. Smith J. Canine prostatic disease: a review of anatomy, pathology, diagnosis and treatment. *Journal of Theriogenology*. 2008;70:375-383.
17. Gelet A, Chapelon JY, Margonari J, et al. Prostatic tissue destruction by HIFU: experimentation on canine prostate. *J Endourol*. 1993;7(3):249-253.
18. Foster RS, Bihle R, Sanghvi N, et al. Production of prostatic lesions in canines using transrectally administered HIFU. *Eur Urol*. 1993;23:330-336.
19. Xavier R, Soulie M, Chartier-Kastlert E, et al. High-intensity focussed ultrasound in prostate cancer; a systematic literature review of the French association of urology. *BJU Int*. 2008;101:1205-1213.
20. Larson TR. Rationale and assessment of minimally invasive approaches to benign prostatic hyperplasia therapy. *Urology*. 2002; 59(2);Suppl 1:12-16.

21. Reike V, Butts PK. MR thermometry. *J Magn Reson Imaging*. 2008;27:376-390.
22. de Seneville BD, Mougnot C, Quesson B, et al. MR thermometry for monitoring tumor ablation. *Eur Radiol*. 2007;2401-2410.
23. Lafon C, Melodelima D, Salomir R, et al. Interstitial devices for minimally invasive thermal ablation by high-intensity ultrasound. *Int J Hyperthermia*. 2007;23(2):153-163.
24. Haar GT, Coussios C. High intensity focussed ultrasound: physical principles and devices. *Int J Hypertherm*. 2007;23(2):89-104.
25. Rouviere O, Souchon R, Salomir R, et al. Transrectal high-intensity focused ultrasound ablation of prostate cancer: effective treatment requiring accurate imaging. *Eur J Radiol*. 2007;63:317-327.
26. Burtnyk M, Chopra R, Bronskill MJ. Qualitative analysis of 3-D conformal MRI-guided transurethral ultrasound therapy of the prostate: theoretical simulations. *Int J Hyperthermia*. 2009;25(2):116-131.
27. Thüroff S, Kiel HJ, Knauer K, et al. High intensity focused ultrasound (HIFU) in prostate cancer—side effects after 1000 treatments in 8 years. *Eur Urol Suppl*. 2005;4:82.